

PROCEEDINGS OF SPIE

SPIDigitalLibrary.org/conference-proceedings-of-spie

Small uncooled bolometers with a broad spectral response

Francis Généreux, Bruno Tremblay, David Gay, Sebastien Deshaies, Martin Briand, et al.

Francis Généreux, Bruno Tremblay, David Gay, Sebastien Deshaies, Martin Briand, Michel Poirier, Jean-Sol Caron, Jacques-Edmond Paultre, David Béland, Francis Provençal, Daniel Desbiens, Yan Desroches, Christine Alain, "Small uncooled bolometers with a broad spectral response," Proc. SPIE 10624, Infrared Technology and Applications XLIV, 106241D (29 May 2018); doi: 10.1117/12.2307290

SPIE.

Event: SPIE Defense + Security, 2018, Orlando, Florida, United States

Small uncooled bolometers with a broad spectral response

Francis Généreux*, Bruno Tremblay, David Gay, Sebastien Deshaies, Martin Briand, Michel Poirier, Jean-Sol Caron, Jacques-Edmond Paultre, David Béland, Francis Provençal, Daniel Desbiens, Yan Desroches and Christine Alain.
INO, 2740 Einstein Street, Quebec, Quebec, Canada, G2P 4S4

ABSTRACT

This paper reports the infrared spectral responses of 17 and 35 μm uncooled bolometers fabricated at INO. They are measured by making use of an external readout circuit along with a monochromator. As expected, the spectral absorption strongly depends on the bolometer stack as well as the pixel layout. By proper selection of design parameters, the spectral response can be made flat from 3 to 14 μm without significant deterioration of the detector figure of merit.

Keywords: Infrared, Uncooled, Microbolometer, 17 μm , 35 μm , Gold black, Figure of merit

1. INTRODUCTION

Due to their low weight and low power consumption, uncooled bolometers are particularly well suited for space applications such as land and sea surface temperature monitoring. To be used for efficient detection of high-temperature events or for radiation budget evaluation, bolometers must have a broad spectral response¹⁻⁴. Wide band microbolometer arrays are also important for the development of hyperspectral imagers⁵. Unfortunately, the spectral response of uncooled microbolometers is typically limited by the absorption of the thermistor and supporting layers to a band ranging from 8 to 16 μm . To address this issue, several techniques such as Salisbury screens^{4, 6}, Jaumann absorbers^{7, 8}, metamaterials⁹ and porous materials¹⁰⁻¹³ have been developed. Amongst them, porous materials are particularly promising in achieving wide spectral absorption. For example, spectral absorption extending from the visible wavelength band up to far infrared was successfully demonstrated by adding a layer of gold black atop a linear array of microbolometer with no major increases of the thermal mass¹³.

Despite this wide spectral range, the use of gold black for the development of high resolution infrared uncooled imagers has been hindered by the difficulty of packaging and patterning this porous material. In a recent paper, however, we showed that gold black can be vacuum sealed using a low temperature packaging process¹⁴. We also demonstrated the laser trimming of a bidimensional array of 35 μm pitch microbolometers and produced the first commercially available camera with gold black¹⁴.

In this paper we demonstrate further improvements of our fabrication processes, leading to what we believe is the first 17 μm pitch microbolometer with gold black. This detector should have a flat spectral absorption from visible to above 40 μm , based on specular reflectance measurements. As a proof of concept, we developed a setup to characterize its spectral response in the 3 to 14 μm range. This setup was also used to characterize the spectral absorption of other types of microbolometers with alternative absorption mechanisms, for comparison purposes. The first section describes the setup and methodology used to evaluate the spectral absorption. The spectral absorption characteristics of 17 and 35 μm pitch bolometers is presented next. The spectral response and figure of merit of the 17 μm bolometers with gold black are shown in the last section.

2. METHODOLOGY AND SETUP DESCRIPTION

The spectral responsivity over the wavelength range from 3 to 14 μm was measured with a McPherson 205f monochromator. Figure 4 shows a schematic of the setup used. The radiation from the glow bar was focused on the input slit of the monochromator. A chopper modulating the radiation at 5 Hz was introduced to remove the low frequency noise from the environment. A spectral filter limited the spectral irradiance range and suppressed the contribution from higher diffraction orders. Two gratings were used to cover the whole spectral range of interest. The first grating covers the wavelength range from 3 to 10 μm , while the second grating covers 8 to 14 μm .

*francis.generoux@ino.ca; phone 1 418 657-7006; fax 1 418 657-7009; www.ino.ca

An optical relay of off-axis paraboloid mirrors at the monochromator output was used to maximize the irradiance on the detector. An iris ensured that the signal incident on the detector has a maximum angle corresponding to an F/1 aperture. A ZnSe polarizer oriented at 45° or 135° with respect to the grating axis accounted for the polarization dependence of the bolometer and compensated for the polarization dependent diffraction efficiency of the gratings. The detector was oriented with respect to the polarizer axis in such a way that the polarization of the collimated beam is either parallel or perpendicular to the bolometer y-axis. The y-axis of each design is shown on the SEM pictures of the following sections.

During measurements, the bolometers were mounted in a hermetic package that was dynamically pumped to achieve a vacuum of 1 mT or less. A broadband germanium window provides sufficient transmission for the wavelength range under study. A mechanical shield was used to hide the blind bolometers from the incoming radiation.

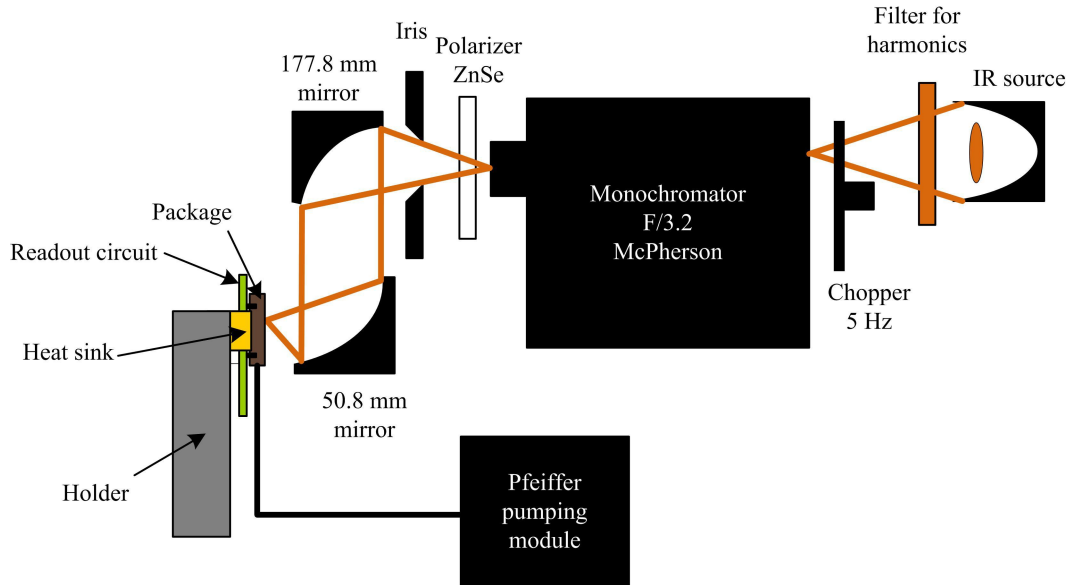


Figure 1. Schematic of the setup used to evaluate the spectral response.

The signal from the bolometer was read by a low noise electronic circuit developed in-house to mimic the behavior of a *ReadOut Integrated Circuits* (ROIC). A schematic of the electronics circuit is shown in Figure 2.

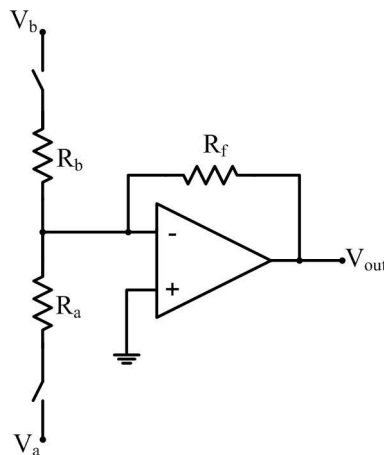


Figure 2. Schematic of the external readout circuit. The subscripts *a*, *b* and *f* stand for active, blind and feedback, respectively.

It consists of a *TransImpedance Amplifier* (TIA) that reads the differential signal from an active bolometer and its blind. The output signal within each pulse was averaged to mimic the behavior of a *Capacitive TransImpedance Amplifier*

(CTIA). The principles behind the signal processing are detailed in a previous paper¹⁵. The RMS signal was evaluated by computing the power spectrum density and integrating over the modulation frequencies of interest, namely from 4 to 6 Hz. The RMS value obtained at each wavelength provides the spectral signal.

2.1 Calibration

Following the spectral signal measurement, the relative output irradiance was measured by replacing the bolometer by a pyroelectric detector. Since the pyroelectric detector is less sensitive than the bolometer, no attempt was made to reduce the pyroelectric surface. The energy incident on the pyroelectric detector was mainly limited by the output slit of the monochromator. The spectral irradiance read by the pyroelectric detector was thus given by the convolution of the input slit with the output slit while in the case of the bolometer it was given by the convolution of the input slit with the bolometer size. Since the bolometer size is much smaller than the output slit, the spectral irradiance read by both detectors was different which may result in erroneous calibration especially close to the water or CO₂ absorption peaks where the spectral irradiance varies rapidly. To overcome this problem, special care was taken to select wavelengths where the spectral irradiance is nearly flat within the resolution band.

The pyroelectric signal was demodulated using a lock-in amplifier. The relative spectral response was obtained by dividing the RMS bolometer spectrum by the RMS pyroelectric spectrum. Since the pyroelectric was underfilled, this approach does provide an absolute calibration of the spectral response. The absolute calibration was achieved by measuring the SiTF and scaling the spectrum adequately. The setup used to measure the SiTF is shown in Figure 3. A 3-inch diameter black-painted aperture is placed in front of a 6-inch black body to restrict the f-number to 1.053. An 8 to 12 μm spectral filter is introduced to limit the incoming spectral irradiance's range. The SiTF was assessed by first plotting the signal as a function of the black body temperature, and then by fitting the slope at the desired temperature. Once the wavelength dependence of the SiTF was known, the spectral absorption was evaluated by fitting the theoretical spectral response computed from the measured values of the bolometer thermal characteristics, namely the activation energy, the thermal conductance and the thermal mass. The accuracy achieved by this approach is about 10%.

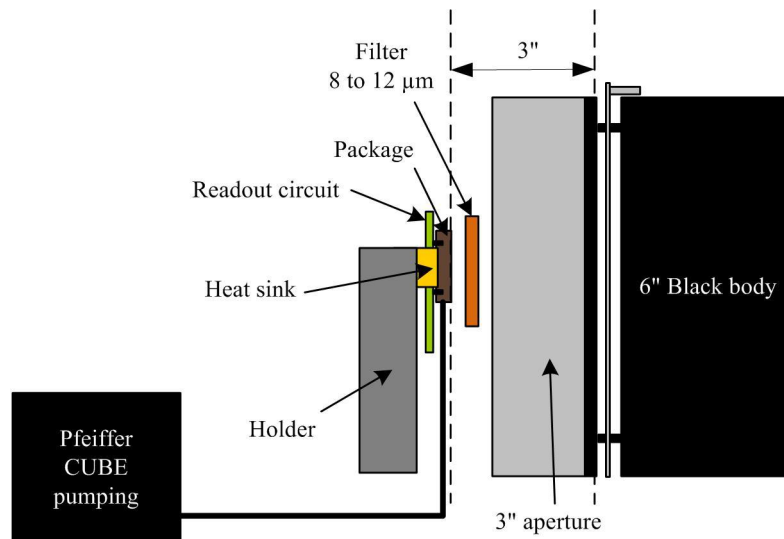


Figure 3. Schematic of the setup used to measure the SiTF in the 8 to 12 μm range.

3. 35 μm PITCH MICROBOLOMETERS

3.1 Standard 35 μm pitch microbolometers

Spectral absorption was first measured on the standard 35 μm bolometers that are commonly used in INO's infrared cameras. Figure 4(a) shows a SEM picture of the bolometer design. It consists of a leg arrangement that provides a large thermal isolation while maintaining a high level of robustness. The interdigital electrodes are used to promote a higher *Temperature Coefficient of Resistance* (TCR) while maintaining a low resistance value. Aside from the leg and bolometer stack, the design does not include any particular features to promote a greater absorption. Figure 4(b) shows the spectral absorption after normalization. As expected, the absorption is relatively small, even in the 8 to 14 μm band,

due to the small platform size. Nonetheless, the overall absorption remains greater than geometrical fill factor would allow, which makes the design worthwhile in terms of figure of merit. For example, the product of the response time over the responsivity is about 20% smaller than the standard L-leg bolometer. However, a significant decrease in the absorption is observed in the 3 to 5 μm region as a result of the low bolometer material absorption in this band.

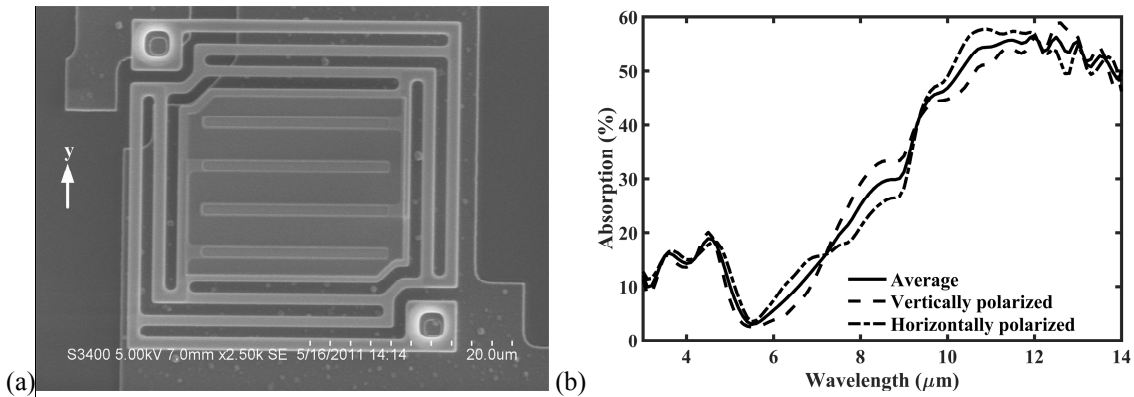


Figure 4. (a) SEM picture of a standard 35 μm pitch microbolometer. (b) Corresponding spectral absorption.

3.2 35 μm pitch microbolometers with metallic absorber

The low absorption in the MWIR can be overcome by using a Salisbury screen, consisting of a metallic absorber placed at a quarter of a wavelength above a perfect mirror. The radiation reflected by the metallic absorber interferes destructively with the reflection of the semi-transparent mirror, resulting in a nearly perfect absorption. In theory, this concept could be used to enhance the absorption in the MWIR band by setting the bolometer platform to a height of about 1 μm . Unfortunately, the refractive index of the bolometer platform contributes to further increase the optical path and leads to an optimal gap that is too small to prevent the platform from collapsing. However, resonances are also present for wavelengths that are $4/3$, $4/5$... times the platform height. By proper selection of the platform height, it is thus possible to match the first resonance at 10 μm and the second resonance at about 4 μm as shown by Figure 5(a). Figure 5(b) shows the spectral absorption measured on a 35 μm bolometer having this optimized stack. A similar stack is currently implemented on the 512x3 FPA in support of the CWFMS mission⁴. A SEM picture of a 35 μm pitch microbolometer with metallic absorber is displayed in Figure 6.

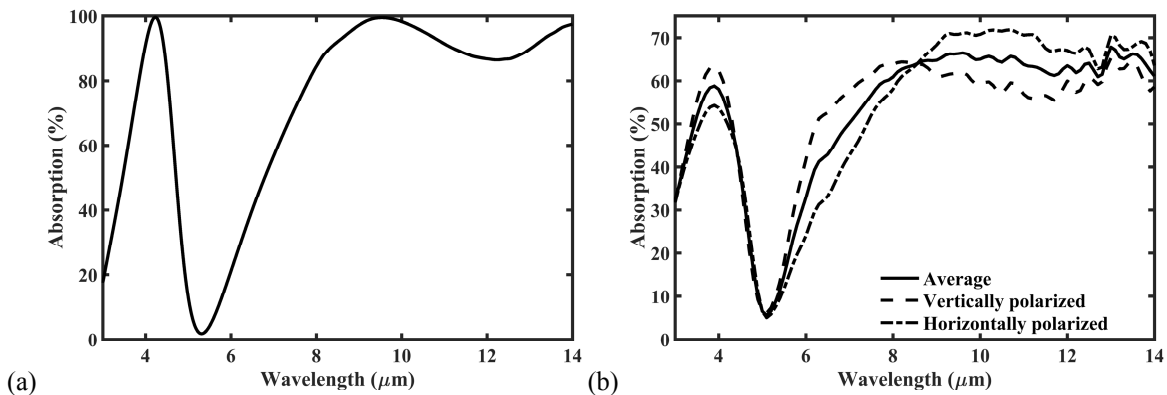


Figure 5. (a) Theoretical absorption spectral absorption based on normal angle of incidence. (b) Measured spectral absorption.

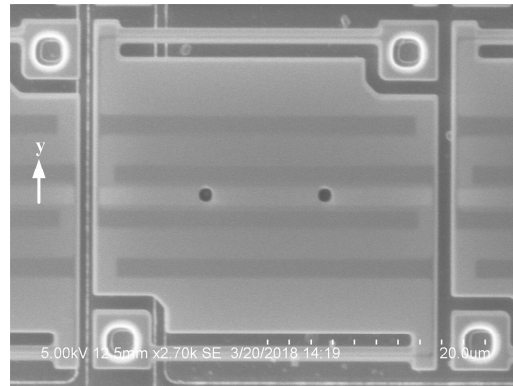


Figure 6. SEM picture of a 35 μm pitch microbolometer with metallic absorber.

As predicted by the model, the spectral absorption shows an absorption peak at about 4 μm as well as a broad absorption in the 7 to 14 μm range. Interestingly, both bands share about the same average amplitude. The polarization dependence is also small. There is still a valley at about 5.1 μm which prevents the realization of a flat spectral absorption through the infrared. Similar oscillations are also predicted by the model in the visible band. Although multiple Jaumann absorbers could be implemented to improve the flatness of the spectral absorption in the 3 to 14 μm region^{7,8}, the absorption at short wavelengths remains limited by the multiple oscillations. The estimated figure of merit for this design is about the same as per standard 35 μm pitch microbolometer.

3.3 35 μm pitch microbolometers with gold black

Unlike Salisbury screens, gold black does not show significant spectral oscillations. Its absorption is also nearly independent of the leg arrangement underneath the gold black. Using the effective medium approximation, it can be described as a uniform layer with optical properties linked to the gold black density¹⁰. If the porosity is sufficiently large, the refractive index gets close to 1 and the incident radiation undergoes almost no reflection. All the incident light is absorbed by the gold black layer, provided that the extinction coefficient value is sufficiently large and that the layer is sufficiently thick for the wavelengths to interfere inside the material. This criterion corresponds more or less to one fourth of the maximum wavelength to be absorbed. The absorption typically extends from the UV to 100 μm wavelength range for a gold black thickness of 25 μm . We used this gold black material for deposition over our standard 35 μm bolometer design. Figure 7(b) illustrates the measured spectral absorption. The absorption is nearly flat over the whole spectral range showing that the leg arrangement, along with the interdigital electrode has little influence on the spectral absorption. The figure of merit value is also low, namely 110 $\text{mK}\cdot\text{ms}$, as was reported in a previous communication¹⁵. The amplitude of the absorption is mainly limited by the laser trimming resolution which contributes to reducing the fill factor.

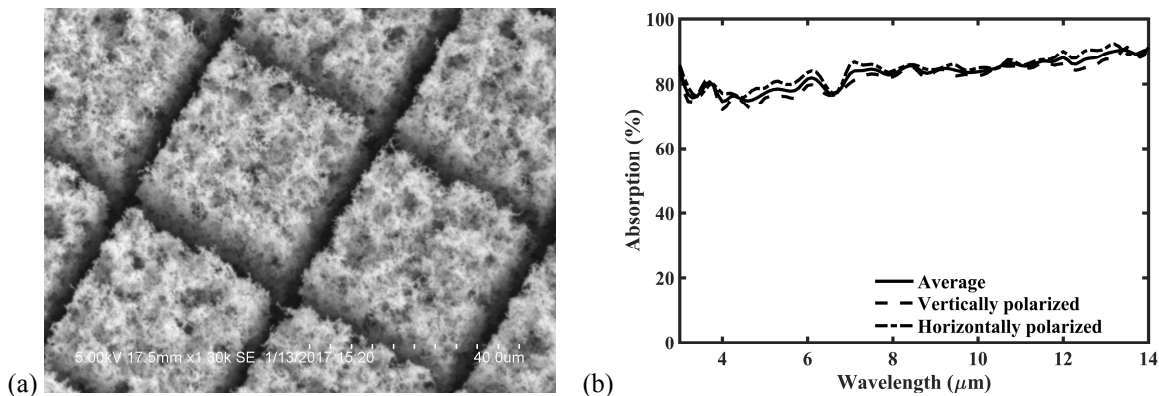


Figure 7. (a) SEM picture of a 35 μm pitch microbolometer with gold black. (b) Corresponding spectral absorption.

4. 17 μm PITCH MICROBOLOMETERS

4.1 Standard 17 μm pitch microbolometers

Figure 8(a) shows a SEM picture of INOs standard 17 μm pitch microbolometers.

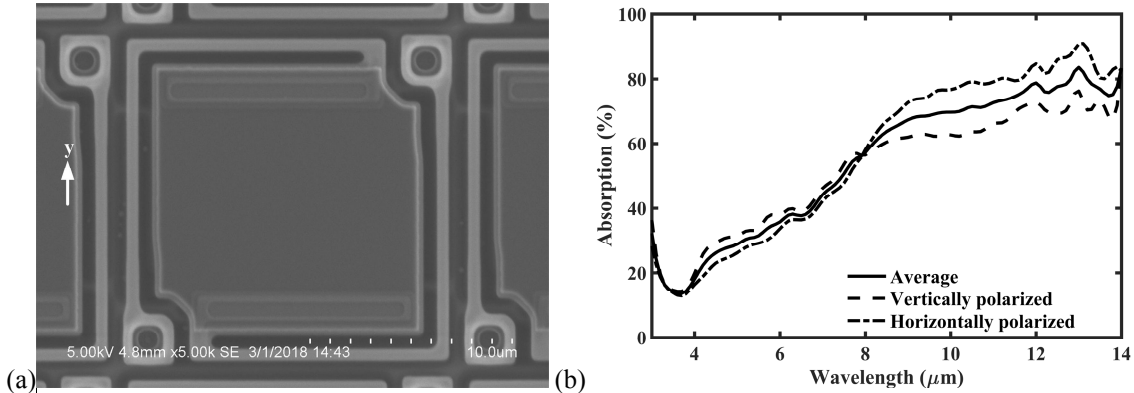


Figure 8. (a) SEM picture of a 17 μm pitch microbolometer. (b) Corresponding spectral absorption.

Compared with the 35 μm pitch microbolometers, this design has a greater fill factor to preserve a low $1/f$ noise coefficient which becomes increasingly important as the pixel pitch is decreased. The stack was also adapted to improve the absorption in the 8 to 12 μm band. Figure 8(b) shows the spectral absorption. As expected, the absorption is greater in the 8 to 12 μm range than for the standard 35 μm pitch microbolometer. Nonetheless, the spectral absorption still shows a significant decrease in the 3 to 5 μm range, although it occurs only at a shorter wavelengths which results in a greater effective absorption. The spectral response shows some polarization dependence, which may be due to the lack of invariance for a rotation of 90° .

4.2 Standard 17 μm pitch microbolometers with gold black

Gold black was deposited atop the 17 μm pitch microbolometer to flatten its spectral absorption. A thinner layer of gold black was deposited to obtain narrower trenches by laser trimming, the trench width being limited by the waist and the Rayleigh distance of the laser beam. Figure 9 shows the specular reflectance of the gold black with reduced thickness. The reflectance remains smaller than 5% up to 35 μm , which is sufficient for most targeted applications.

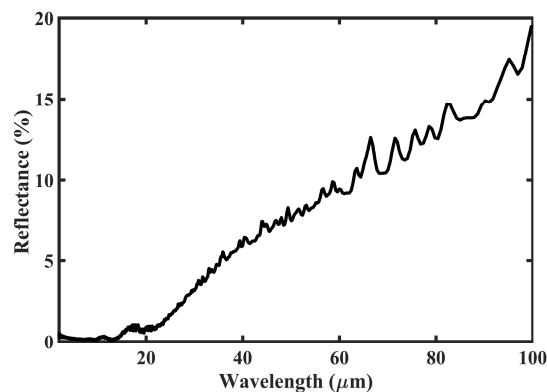


Figure 9. Specular reflectance of gold black with reduced thickness deposited on a gold film. The incidence angle is 10° .

Figure 10(a) shows a SEM picture of the laser trimmed bolometers. The trench width is about 2 times narrower than for the 35 μm pitch microbolometers. Figure 10(b) displays the spectral absorption from 3 to 14 μm . The absorption spectrum is flat over the band and it should be flat from the visible wavelength range to 40 μm , based on the above

specular reflectance measurement of the corresponding gold black layer. The polarization dependence is within the measurement error.

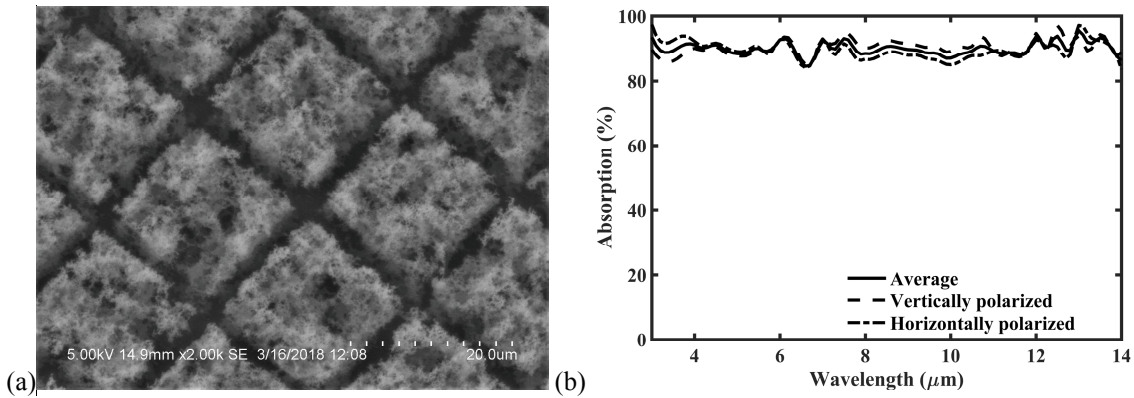


Figure 10. (a) SEM picture of the 17 μm pitch microbolometer with gold black. (b) Corresponding spectral absorption.

To verify the effect of gold black on the figure of merit, the *Noise Equivalent Temperature Difference* (NETD) and the response time were measured for this specific bolometer design using the approach described in a previous communication¹⁵. The settings used for this measurement are shown in Table 1. Figure 11 shows the NETD histogram along with the response time. The median NETD value is 17.6 mK and the response time is 13.8 ms, corresponding to figure of merit of 244 mK*ms. Interestingly, this value is fairly close to the value reported for 17 μm without gold black and is in line with the current state of the art. Further improvement of the figure of merit could be achieved by using a more resistive VO_x to improve TCR and by decreasing the bolometer platform area as per standard 35 μm pitch microbolometer.

Table 1. Settings used for the characterization of 17 μm pitch microbolometers with gold black absorber.

Settings	Values
Frame rate	30 Hz
V_a	-1.5 V
V_b	4.411 V
Number of blind bolometers	3
Integration time	83.2 μs
Staring time	1 s
Number of pulse trains	60
R_f	200 k Ω
Biasing time	100 μs

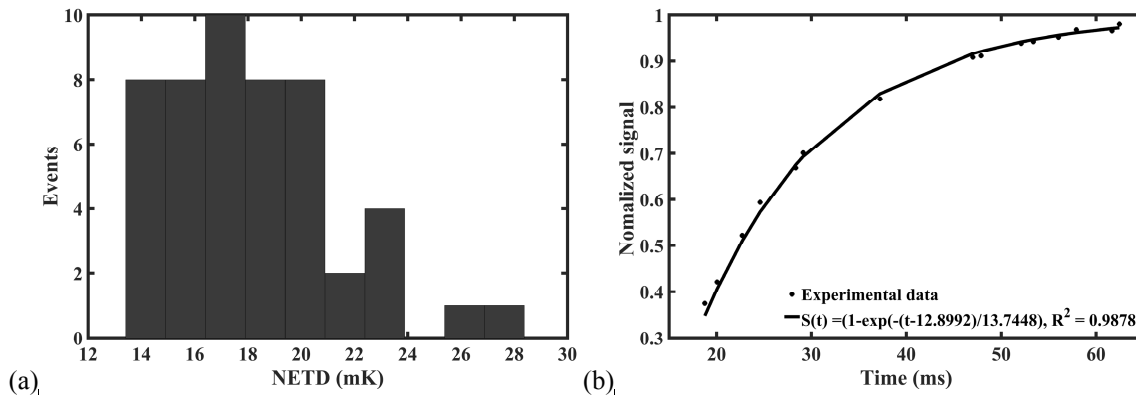


Figure 11. (a) NETD histogram for 17 μm pitch microbolometers with gold black. (b) Temporal response after shutter opening.

5. CONCLUSIONS

The spectral absorption of 17 and 35 μm pitch microbolometers fabricated at INO was measured using an external readout circuit along with a monochromator. The results show that the spectral absorption of standard bolometers is not flat, and indeed shows a large decrease in the 3 to 5 μm spectral region. Although a properly tuned Salisbury screen helps in improving the absorption of 35 μm pitch microbolometers in the 3 to 5 μm range, the spectral absorption still shows significant oscillations. Spectrally flat absorption was achieved by depositing gold black on 17 and 35 μm pitch microbolometers. The measured figures of merit for 17 and 35 μm pitch microbolometers are respectively 110 and 244 $\text{mK}\cdot\text{ms}$, which compare well with the values reported without gold black. Work is currently underway to characterize the spectral absorption of gold black coated 12 μm pitch microbolometers.

ACKNOWLEDGMENTS

A portion of the work presented in this paper has been funded by the European Space Agency (ESA Contract 400105063/12/NL/NA).

REFERENCES

- [1] K. Wallace, N. Wright, D. Spilling *et al.*, "The broadband radiometer on the EarthCARE spacecraft," Proc. SPIE 7453, 74530H (2009).
- [2] M. Allard, L. Martin, C. Proulx *et al.*, "Current status of the EarthCARE BBR detectors development," Proc. SPIE 8176, 81761E (2011).
- [3] L. N. Phong, A. Alazzam, M. G. Daly *et al.*, "Net flux sensors for the measurement of Mars surface radiation budget," Proc. SPIE 8252, 82520A (2012).
- [4] L. N. Phong, F. Picard, J.-E. Paultre *et al.*, "Uncooled midwave infrared sensors for spaceborne assessment of fire characteristics," Proc. SPIE 10116, 101160N (2017).
- [5] D. Béland, H. Spisser, D. Dufour *et al.*, "Portable LWIR hyperspectral imager based on MEMS Fabry-Perot interferometer and broadband microbolometric detector array," Proc. SPIE 10545, 105450S (2018).
- [6] J. L. Tissot, C. Trouilleau, A. Crastes *et al.*, "Uncooled microbolometer detector: recent development at Ulis," Opto-Electronics Review, 14(1), 25-32 (2006).
- [7] C. Li, C.-J. Han, and G. D. Skidmore, "Overview of DRS uncooled VOx infrared detector development," Optical Engineering 50(6), 061017 (2011).
- [8] C. Li, G. D. Skidmore, C. Howard *et al.*, "Recent development of ultra small pixel uncooled focal plane arrays at DRS," Proc. SPIE 6542, 65421Y (2007).
- [9] J. J. Talghader, A. S. Gawarikar, and R. P. Shea, "Spectral selectivity in infrared thermal detection," Light: Science & Applications, 1(8), e24 (2012).

- [10] W. Becker, R. Fetting, and W. Ruppel, "Optical and electrical properties of black gold layers in the far infrared," *Infrared Physics & Technology*, 40(6), 431-445 (1999).
- [11] E. M. Smith, D. Panjwani, J. Ginn *et al.*, "Enhanced performance of VO_x-based bolometer using patterned gold black absorber," *Proc. SPIE* 9451, 94511I (2015).
- [12] S. Ilias, P. Topart, C. Larouche *et al.*, "Deposition and characterization of gold black coatings for thermal infrared detectors," *Proc. SPIE* 7750, 77501J (2010).
- [13] C. Proulx, F. Williamson, M. Allard *et al.*, "The EarthCARE broadband radiometer detectors," *Proc. SPIE* 7453, 74530S (2009).
- [14] B. Fisette, M. Tremblay, H. Oulachgar *et al.*, "Novel vacuum packaged 384x288 broadband bolometer FPA with enhanced absorption in 3-14 um wavelength range," *Proc. SPIE* 10177, 101771R (2017).
- [15] F. Génèreux, B. Tremblay, M. Girard *et al.*, "On the figure of merit of uncooled bolometers fabricated at INO," *Proc. SPIE* 9819, 98191U (2016).